Hindawi Publishing Corporation
EURASIP Journal on Image and Video Processing
Volume 2010, Article ID 517861, 13 pages
doi:10.1155/2010/517861

Research Article

Real-Time Multiview Recognition of Human Gestures by Distributed Image Processing

Toshiyuki Kirishima,[1] Yoshitsugu Manabe,[1] Kosuke Sato,[2] and Kunihiro Chihara[1]

[1] *Graduate School of Information Science, Nara Institute of Science and Technology, 8916-5 Takayama-cho, Ikoma-shi, Nara 630-0101, Japan*
[2] *Graduate School of Engineering Science, Osaka University, 1-3 Machikaneyama-cho, Toyonaka-shi, Osaka 560-8531, Japan*

Correspondence should be addressed to Toshiyuki Kirishima, kirishima@is.naist.jp

Received 18 March 2009; Accepted 3 June 2009

Academic Editor: Ling Shao

Since a gesture involves a dynamic and complex motion, multiview observation and recognition are desirable. For the better representation of gestures, one needs to know, in the first place, from which views a gesture should be observed. Furthermore, it becomes increasingly important how the recognition results are integrated when larger numbers of camera views are considered. To investigate these problems, we propose a framework under which multiview recognition is carried out, and an integration scheme by which the recognition results are integrated online and in realtime. For performance evaluation, we use the ViHASi (Virtual Human Action Silhouette) public image database as a benchmark and our Japanese sign language (JSL) image database that contains 18 kinds of hand signs. By examining the recognition rates of each gesture for each view, we found gestures that exhibit view dependency and the gestures that do not. Also, we found that the view dependency itself could vary depending on the target gesture sets. By integrating the recognition results of different views, our swarm-based integration provides more robust and better recognition performance than individual fixed-view recognition agents.

1. Introduction

For the symbiosis of humans and machines, various kinds of sensing devices will be either implicitly or explicitly embedded, networked, and cooperatively function in our future living environment [1–3]. To cover wider areas of interest, multiple cameras will have to be deployed. In general, gesture recognizing systems that function in real world must operate in real-time, including the time needed for event detection, tracking, and recognition. Since the number of cameras can be very large, distributed processings of incoming images at each camera node are inevitable in order to satisfy the real-time requirement. Also, improvements in recognition performance can be expected by integrating responses from each distributed processing component. But it is usually not evident how the responses should be integrated. Furthermore, since a gesture is such a dynamic and complex motion, single-view observation does not necessary guarantee better recognition performance. One needs to know from which camera views a gesture should be observed in order to quantitatively determine the optimal camera configuration and views.

2. Related Work

For the visual understanding of human gestures, a number of recognition approaches and techniques have so far been proposed [4–10]. Vision-based approaches usually employ a method that estimates a gesture class to which the incoming image belongs by introducing pattern recognition techniques. To make the recognition system more reliable and usable in our activity spaces, many approaches that employ multiple cameras are actively developed in recent years. These approaches can be classified into the geometry-based approach [11] and the appearance-based approach [12]. Since the depth information can be computed by using multiple camera views, the geometry-based approach can estimate three-dimensional (3D) relationship between the human body and its activity spaces [13]. For example, multiple person's actions such as walking including its path

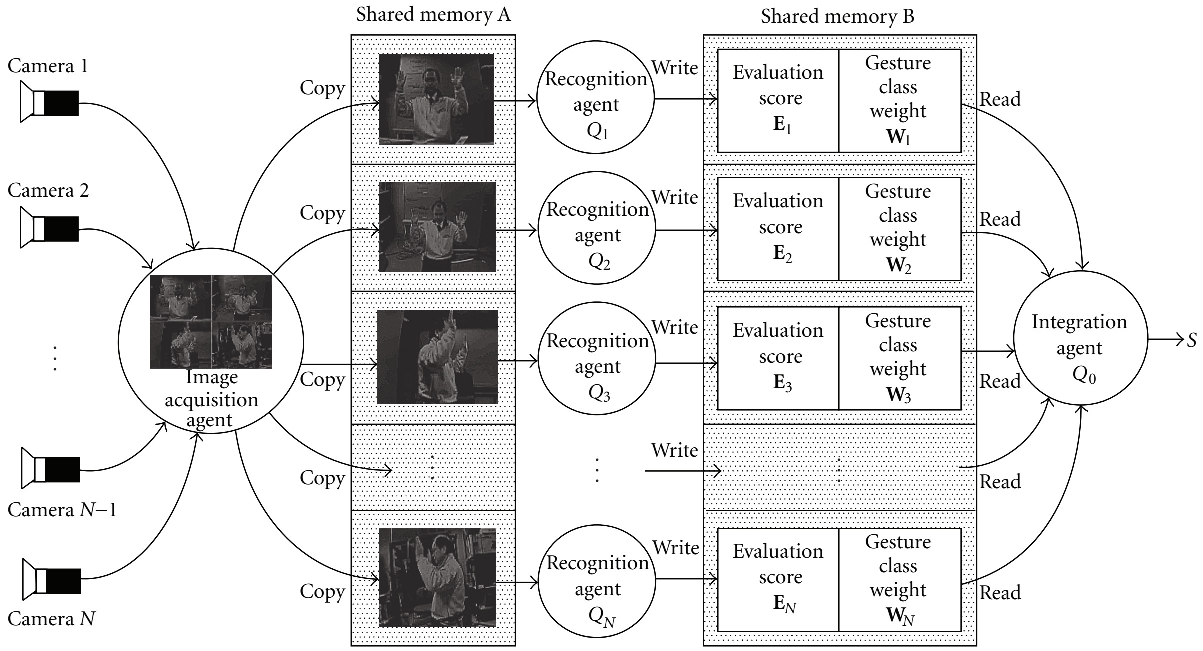

Figure 1: The proposed framework for multiview gesture recognition.

can be reliably estimated [2, 10]. On the other hand, the appearance-based approach usually focuses on more detailed understanding of human gestures. Since a gesture is a spatiotemporal event, spatial- and temporal-domain problems need to be considered at the same time. In [14], we have investigated the temporal-domain problems on gesture recognition and suggested that the recognition performance can depend on image sampling rate. Although there are some studies on view selection problems [15, 16], they do not deal with human gestures, and how the recognition results should be integrated when larger numbers of camera views are available is not studied. This means that most of the multiview gesture recognition system's actual camera configuration and views are determined empirically. There is a fundamental need to evaluate the recognition performance depending on camera views. To deal with the above-mentioned problems, we propose (1) a framework under which recognition is performed using multiple camera views (2) an integration scheme by which the recognition results are integrated on-line and in real-time. The effectiveness of our framework and an integration scheme is demonstrated by the evaluation experiments.

3. Multiview Gesture Recognition

3.1. Framework. A framework for multiview gesture recognition is illustrated in Figure 1. Image acquisition agent obtains a synthesized multiview image that is captured by multiple cameras and stores each camera view image in the shared memory corresponding to each recognition agent. Each recognition agent controls its processing frame rate autonomously and resamples the image data in the shared memory at the specified frame rate. In this paper, we assume a model in which each recognition agent performs recognition and outputs the following results for each gesture class: evaluation score matrix $\mathbf{E}_n$ and gesture class weight matrix $\mathbf{W}_n$,

$$\mathbf{E}_n = (e_{n1}, e_{n2}, e_{n3}, \ldots, e_{ni}, \ldots, e_{nM}), \tag{1}$$

$$\mathbf{W}_n = (w_{n1}, w_{n2}, w_{n3}, \ldots, w_{ni}, \ldots, w_{nM}). \tag{2}$$

Here, M denotes the maximum number of target gestures. These results are updated in the specific data area in shared memory B corresponding to each recognition agent. Then, the integration agent Q_0 reads out the evaluation score matrix $\mathbf{E}_n$ and the gesture class weight matrix $\mathbf{W}_n$ and computes an integrated score for each gesture class as follows. For the i_{th} $(i = 1, 2, \ldots, M)$ gesture, the integrated score S_i, which represents the swarm's response, is computed by (3)

$$S_i = \prod_{n=1}^{N} e_{ni} w_{ni}. \tag{3}$$

Here, N denotes the maximum number of recognition agents. Finally, the integrated score matrix $\mathbf{S}$ is given as following:

$$\mathbf{S} = (S_1, S_2, \ldots, S_i, \ldots, S_M). \tag{4}$$

The input image is judged to belong to the gesture class for which the integrated score S_i becomes the maximum.

3.2. Recognition Agent. In this paper, each gesture recognition agent is created by our method that is proposed in [17] since it can perform recognition at an arbitrary frame rate. In the following subsections, it is briefly explained

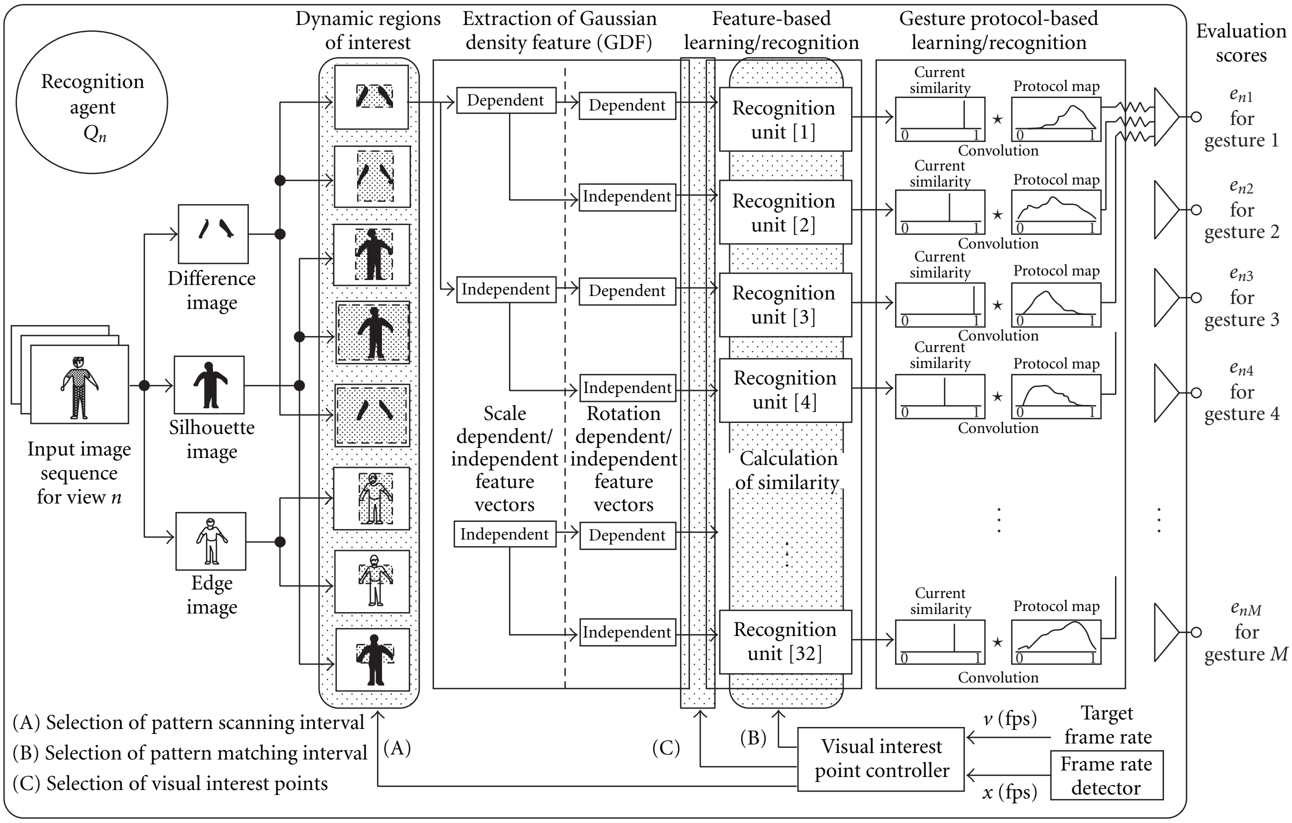
Recognition agent Q_n
Input image sequence for view n
Difference image
Silhouette image
Edge image
Dynamic regions of interest
Extraction of Gaussian density feature (GDF)
Dependent
Independent
Scale dependent/ independent feature vectors
Rotation dependent/ independent feature vectors
Feature-based learning/recognition
Recognition unit [1]
Recognition unit [2]
Recognition unit [3]
Recognition unit [4]
Recognition unit [32]
Calculation of similarity
Gesture protocol-based learning/recognition
Current similarity
Protocol map
Convolution
Evaluation scores
e_{n1} for gesture 1
e_{n2} for gesture 2
e_{n3} for gesture 3
e_{n4} for gesture 4
e_{nM} for gesture M
(A) Selection of pattern scanning interval
(B) Selection of pattern matching interval
(C) Selection of visual interest points
(A)
(B)
(C)
Visual interest point controller
v (fps)
Target frame rate
x (fps)
Frame rate detector

Figure 2: Processing flow diagram of our recognition agent.

how our method performs recognition and how to obtain the evaluation score matrix $\mathbf{E}_n$ and the gesture class weight matrix $\mathbf{W}_n$. As shown in Figure 2, our framework takes a multilayered hierarchical approach that consists of three stages of gestural image processing: (1) feature extraction, (2) feature-based learning/matching, and (3) gesture protocol-based learning/recognition. By applying three kinds of feature extraction filters to the input image sequence, a difference image, a silhouette image, and an edge image are generated. Using these feature images, regions of interest are dynamically set frame by frame. Regarding the binary image in each dynamic region of interest, the following feature vectors are computed based on the feature vector $s_\varepsilon(\theta)$ given by (5): (1) a feature vector that depends on both scale and rotation, (2) a feature vector that depends on scale but not on rotation, (3) a feature vector that depends on rotation but not on scale, and (4) a feature vector that does not depend on both scale and rotation.

Let $P_\tau(r,\theta)$ represent the given binary image in a polar coordinate system:

$$s_\varepsilon(\theta) = R\frac{\sum_r P_\tau(r,\theta)\exp\left\{-a(r-\phi)^2\right\}}{\sum_r P_\tau(r,\theta)}, \tag{5}$$

where, θ is the angle, R is the radius of the binary image, and r is the distance from a centroid of the binary image. And a is a gradient coefficient that determines the uniqueness of the feature vector, and ϕ is a phase term that is an offset value. In the learning phase, obtained feature vectors are stored as a reference data set. In the matching phase, obtained feature vectors are compared with the feature vectors in the reference data set, and each recognition unit outputs similarity by (6)

$$\text{Similarity} = 1 - \frac{d_l^{(k_i)}}{\text{Max}\left(d_l^{(g)}\right)}, \tag{6}$$

where g refers to an arbitrary number of reference data set, and $d_l^{(k_i)}$ is the minimum distance between the given feature vector and the reference data set. Max() is a function that returns the maximum value.

Then, in order to recognize human gestures with more flexibility, protocol learning is conducted. The purpose of protocol learning is to let the system focus on visual features of greater significance by using a sequence of images that is provided as belonging to the identical gesture class. In the protocol learning, larger weights are given to the visual features that are spatiotemporally consistent. Based on the sequence of similarity, likelihood functions are estimated and stored as a protocol map assuming the distribution function to be Gaussian. Based on the protocol map for recognition agent Q_n, each component of $\mathbf{W}_n$ in (2) is given by (7)

$$w_{ni} = \frac{L}{\sum_{l=1}^{L}\Omega_{nl}}, \tag{7}$$

where L is the maximum number of visual interest points, and Ω_{nl} is the weight for each visual interest point of recognition agent Q_n. In the recognition phase, each component

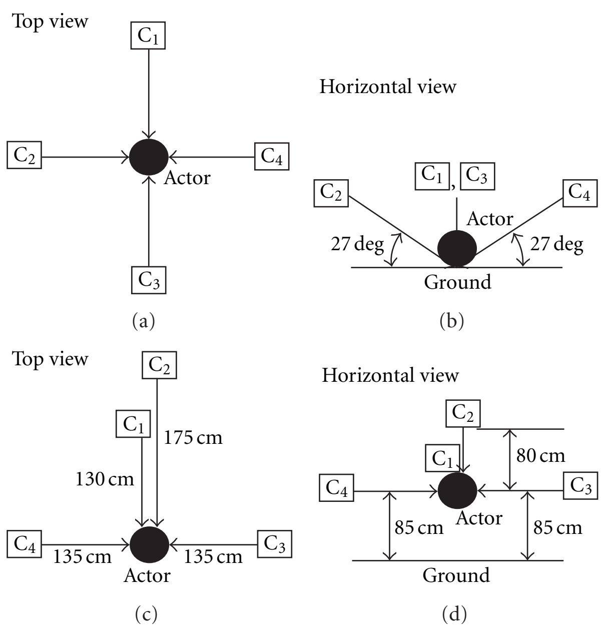

(a) (b) (c) (d)

Figure 3: Camera configuration.

Camera 1 (C_1)	Camera 2 (C_2)
Camera 3 (C_3)	Camera 4 (C_4)

Figure 4: Camera view allocation.

of $\mathbf{E}_n$ in (1) is computed, which is the sum of convolution between the similarity and each protocol map as illustrated in Figure 2. The input image is judged to belong to the gesture class that returns the biggest sum of convolution.

3.3. Frame Rate Control Method. Generally, the actual frame rate of gesture recognition systems depends on (1) duration of each gesture, (2) number of gesture classes, and (3) performance of the implemented system. In addition, recognition systems must deal with slow and unstable frame rate caused by the following factors: (1) increase in pattern matching cost, (2) increased number of recognition agents, and (3) load fluctuations in the third party processes under the same operating systems environment.

In order to maintain the specified frame rate, a feedback control system is introduced as shown in the bottom part of Figure 2, which dynamically selects the magnitude of processing load. The control inputs are pattern scanning interval S_k, pattern matching interval RS_k, and the number of effective visual interest points N_{vip}. Here, S_k refers to the jump interval in scanning the feature image, and RS_k refers to the loop interval in matching the current feature vector with feature vectors in the reference data set. The controlled variable is the frame rate x (fps), and v (fps) is the target frame rate. The frame rate is stabilized by controlling the load of the recognition modules. Control inputs are determined in accordance with the response from frame rate detector. The feedback control is applied as long as the control deviation does not fall within the minimal error range.

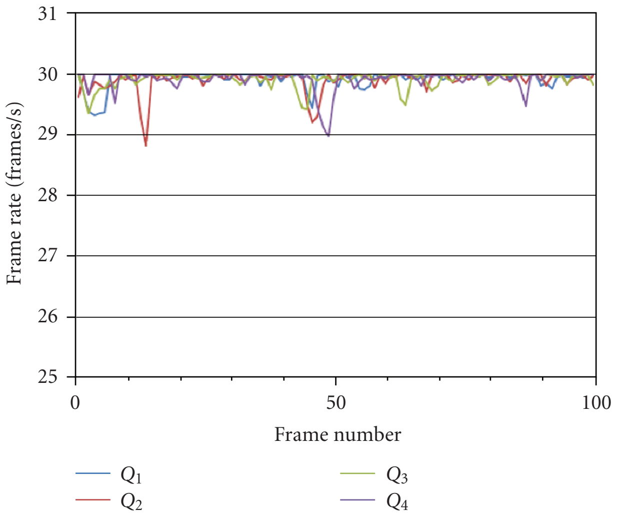

Figure 5: Fluctuation of the processing frame rate.

4. Experiments

The experiments are conducted on a personal computer (Core 2 Duo, 2 GHz, 2 GB Memory) under the Linux operating system environment.

4.1. Experiment I. We introduce publicly available ViHASi (Virtual Human Action Silhouette) [18] image database in order to evaluate the proposed approach from an objective perspective. The ViHASi image database provides binary silhouette images of virtual CG actor's multiview motion that are captured at 30 fps in the PGM (Portable Gray Map) format. To investigate view dependency for different kinds of gestures, 18 gestures in the ViHASi image database are divided into three groups: Groups (A, B, and C) as shown in Table 1. In this experiment, we use synthesized multiview images observed from four different views although the number of camera views is not restricted in our approach. The camera configuration of ViHASi image database is illustrated in Figures 3(a) and 3(b). Allocation of each camera view is illustrated in Figure 4. For quick reference, trace images of each gesture are shown in Figure 22.

In this experiment, the image acquisition agent reads out the multiview image, and each view image is converted into an 8-bit gray scale image whose resolution is 80 by 60 dots and then stored in the shared memory area. Each recognition agent reads out the image and performs the recognition on-line and in real-time. The experiments are carried out according to the following procedures.

(Procedure I-1). Launch four recognition agents (Q_1, Q_2, Q_3, and Q_4), then perform the protocol learning on six kinds of gestures in each group. In this experiment, the recognition

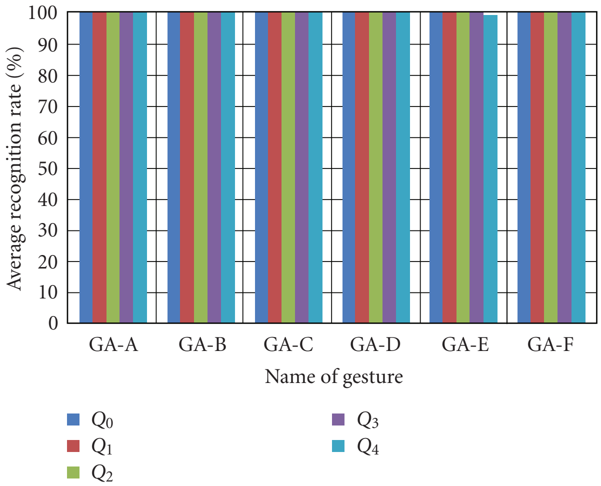

Figure 6: Group A.

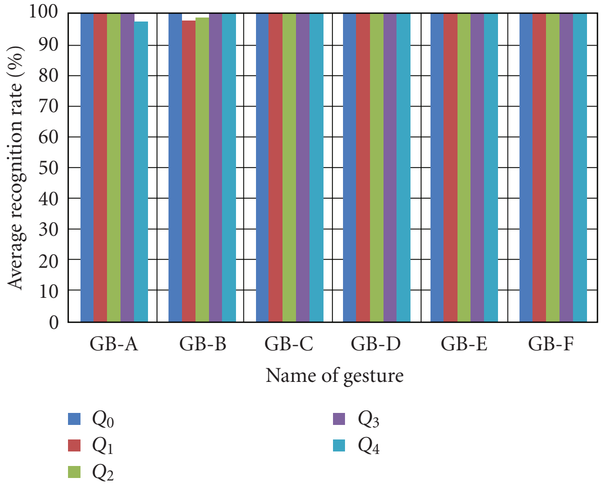

Figure 7: Group B.

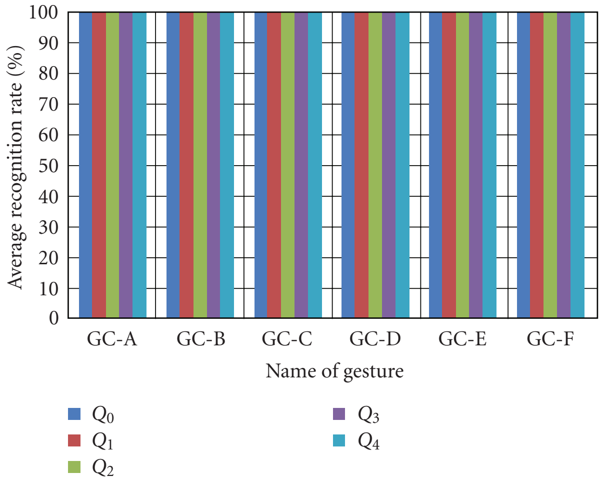

Figure 8: Group C.

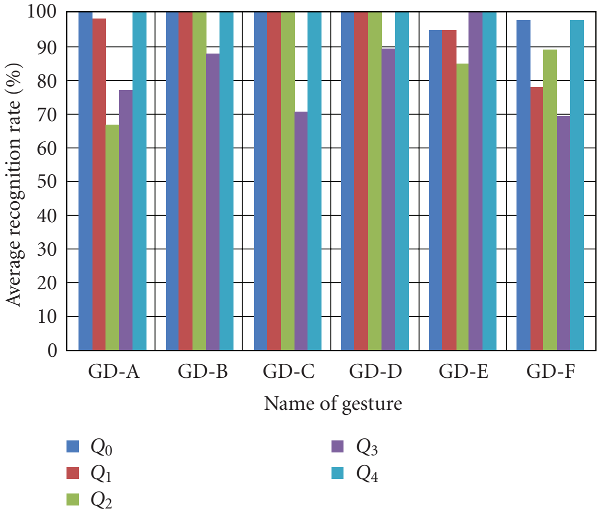

Figure 9: Group D.

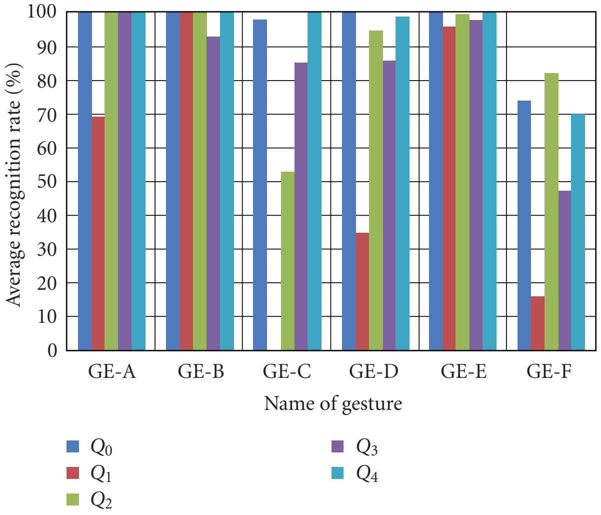

Figure 10: Group E.

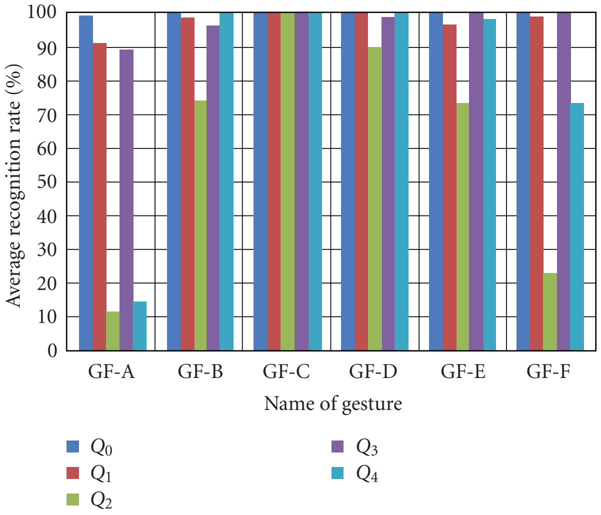

Figure 11: Group F.

Table 1: Target gesture sets (Part I).

Group A	
Name	Description
GA-A	HangOnBar
GA-B	JumpGetOnBar
GA-C	JumpOverObject
GA-D	JumpFromObject
GA-E	RunPullObject
GA-F	RunPushObject
Group B	
Name	Description
GB-A	RunTurn90Left
GB-B	RunTurn90Right
GB-C	HeroSmash
GB-D	HeroDoorSlam
GB-E	KnockoutSpin
GB-F	Knockout
Group C	
Name	Description
GC-A	Granade
GC-B	Collapse
GC-C	StandLookAround
GC-D	Punch
GC-E	JumpKick
GC-F	Walk

Table 2: Target gesture sets (Part II).

Group D	
Name	Description
GD-A	today
GD-B	night
GD-C	christmas
GD-D	water
GD-E	dog
GD-F	volley ball
Group E	
Name	Description
GE-A	golf
GE-B	son
GE-C	lung
GE-D	gather
GE-E	sing
GE-F	get angry
Group F	
Name	Description
GF-A	live
GF-B	get tired
GF-C	create
GF-D	drink
GF-E	mistake
GF-F	happy

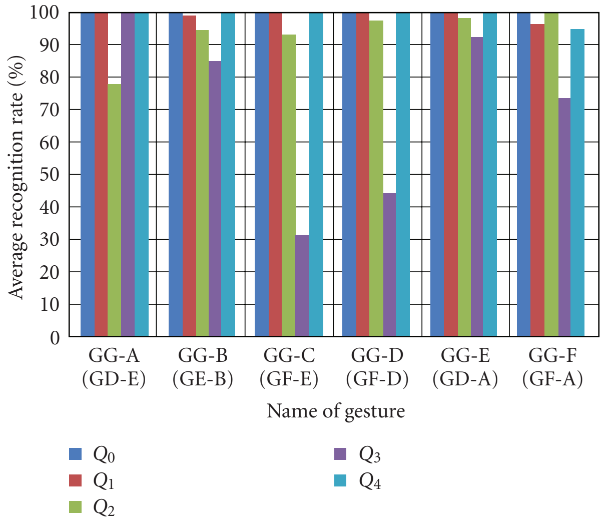

Figure 12: Group G.

agent Q_1 also plays the role of an integration agent Q_0. Since the ViHASi image database does not contain any instances for each gesture, standard samples are also used as training samples in the protocol learning.

(Procedure I-2). The target frame rate of each recognition agent is set to 30 fps. Then, the frame rate control is started.

(Procedure I-3). Feed the testing samples into the recognition system. For each gesture, 10 standard samples are tested.

(Procedure I-4). The integrated score S_i is computed by recognition agent Q_0 based on the evaluation scores in the shared memory B.

The procedures I-3 and I-4 are repeatedly applied to six kinds of gestures in each group. Typical fluctuation curves of the processing frame rate for each recognition agent are shown in Figure 5. As shown in Figure 5, the error of each controlled frame rate mostly falls within 1 fps. The average recognition rates for the gestures in group A are shown in Figure 6, for the gestures in group B are shown in Figure 7, and for the gestures in group C are shown in Figure 8.

4.2. Experiment II. As an original image database, we created a Japanese sign language (JSL) image database that contains 18 gestures in total. For each gesture class, our JSL database contains 22 similar samples, 396 samples in all. From the 22 similar samples, one standard sample and one similar sample are randomly selected for the learning and the remaining 20 samples are used for the test. The images from four CCD cameras are synthesized into single image frame by using a video signal composition device. The camera configuration for our JSL image database is illustrated in Figures 3(c) and 3(d), and the camera view allocation shown in Figure 4 is adopted. The synthesized multiview image is captured by an image capture device and then recorded in the database

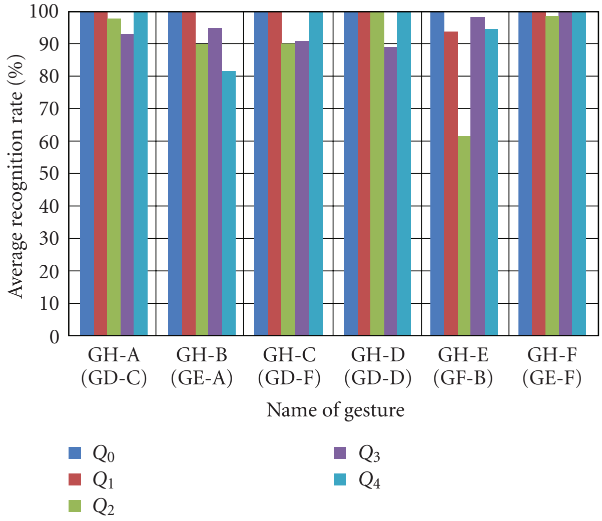

Figure 13: Group H.

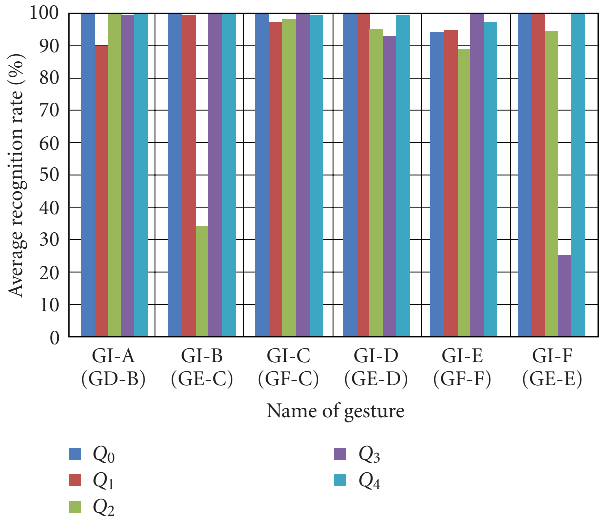

Figure 14: Group I.

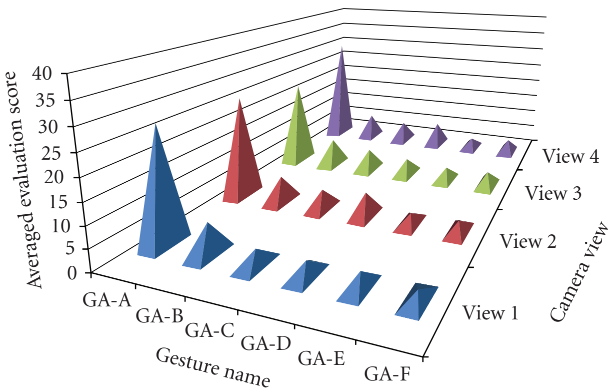

Figure 15: Averaged evaluation scores when the gesture GA-A is input to the system.

Table 3: Target gesture sets (Part III).

Group G

Name	Description
GG-A (GD-E)	dog
GG-B (GE-B)	son
GG-C (GF-E)	mistake
GG-D (GF-D)	drink
GG-E (GD-A)	today
GG-F (GF-A)	live

Group H

Name	Description
GH-A (GD-C)	christmas
GH-B (GE-A)	golf
GH-C (GD-F)	volley ball
GH-D (GD-D)	water
GH-E (GF-B)	get tired
GH-F (GE-F)	get angry

Group I

Name	Description
GI-A (GD-B)	night
GI-B (GE-C)	lung
GI-C (GF-C)	create
GI-D (GE-D)	gather
GI-E (GF-F)	happy
GI-F (GE-E)	sing

Table 4: Average recognition rates for each gesture group in Experiments I, II, and III (%).

Experiment I

Group	Q_0	Q_1	Q_2	Q_3	Q_4	Ave.
A	100.0	100.0	100.0	100.0	99.9	100.0
B	100.0	99.6	99.8	100.0	99.6	99.8
C	100.0	100.0	100.0	100.0	100.0	100.0
Ave.	100.0	99.9	99.9	100.0	99.8	99.9

Experiment II

Group	Q_0	Q_1	Q_2	Q_3	Q_4	Ave.
D	98.8	95.2	90.0	82.4	99.5	93.2
E	95.3	52.5	88.0	84.6	94.8	83.0
F	99.9	97.7	62.3	97.6	81.2	87.7
Ave.	98.0	81.8	80.1	88.2	91.8	88.0

Experiment III

Group	Q_0	Q_1	Q_2	Q_3	Q_4	Ave.
G	99.9	99.1	93.5	71.1	99.2	92.6
H	100.0	98.8	89.6	94.2	95.9	95.7
I	99.1	97.0	85.2	86.3	99.4	93.4
Ave.	99.7	98.3	89.4	83.9	98.2	93.9

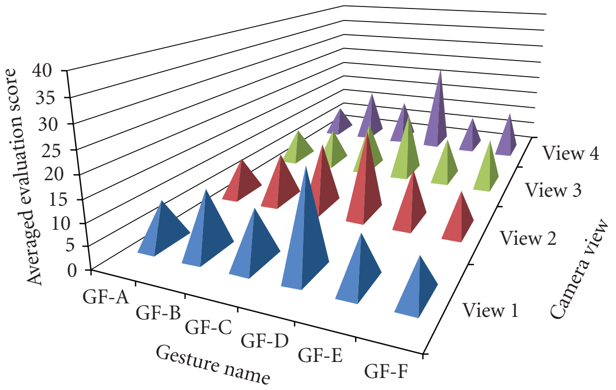

Figure 16: Averaged evaluation scores when the gesture GF-D is input to the system.

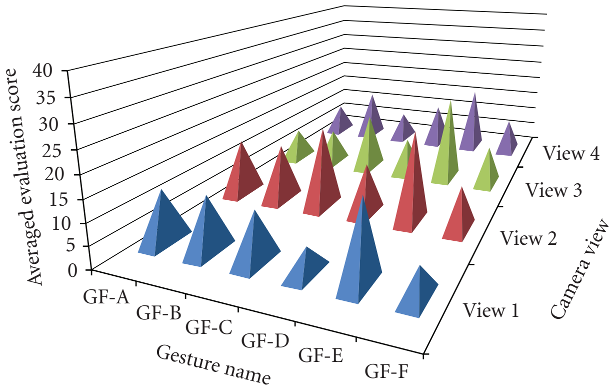

Figure 18: Averaged evaluation scores when the gesture GF-E is input to the system.

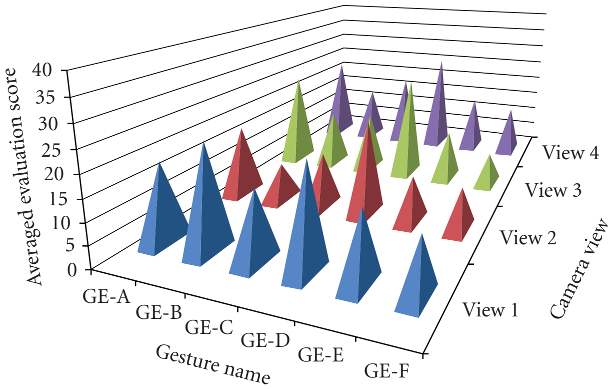

Figure 17: Averaged evaluation scores when the gesture GE-D is input to the system.

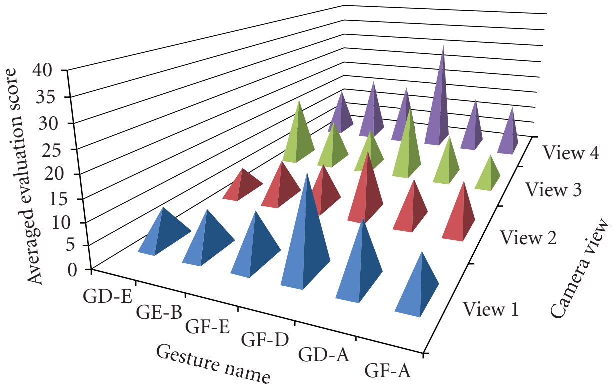

Figure 19: Averaged evaluation scores when the gesture GG-D(GF-D) is input to the system.

in size of 320 by 240 pixels and by 16-bit color (R:5[bit], G:6[bit], B:5[bit]). The actual frame rate is 30 fps since NTSC-compliant image capture device is used. To investigate view dependency for different kinds of gestures, 18 gestures in our database are divided into three groups: Groups (D, E, and F) as shown in Table 2. The trace images of each gesture are shown in Figure 23.

In this experiment, the image acquisition agent reads out the multiview image in the database and converts each camera view image into an 8-bit gray scale image whose resolution is 80 by 60 dots and then stores each gray scale image in the shared memory area. Each recognition agent reads out the image and performs the recognition on-line and in real-time. The experiments are carried out according to the following procedures.

(Procedure II-1). Launch four recognition agents (Q_1, Q_2, Q_3, and Q_4), then perform the protocol learning on six kinds of gestures in each group. In this experiment, the recognition agent Q_1 also plays the role of an integration agent Q_0. As training samples, one standard sample and one similar sample are used for the learning of each gesture.

(Procedure II-2). The target frame rate of each recognition agent is set to 30 fps. Then, the frame rate control is started.

(Procedure II-3). Feed the testing samples into the recognition system. For each gesture, 20 similar samples that are not used in the training phase are tested.

(Procedure II-4). The integrated score S_i is computed by recognition agent Q_0 based on the evaluation scores in the shared memory B.

The procedures II-3 and II-4 are repeatedly applied to six kinds of gestures in each group. The average recognition rates for the gestures in group D are shown in Figure 9, for the gestures in group E are shown in Figure 10, and for the gestures in group F are shown in Figure 11.

4.3. Experiment III. As shown in Table 3, other Groups (G, H, and I) are created by changing the combination of 18 gestures in Groups (D, E, and F). The trace images of each gesture are shown in Figure 23. Then, another experiment is conducted according to the same procedure in Experiment II. The average recognition rates for the gestures in group G

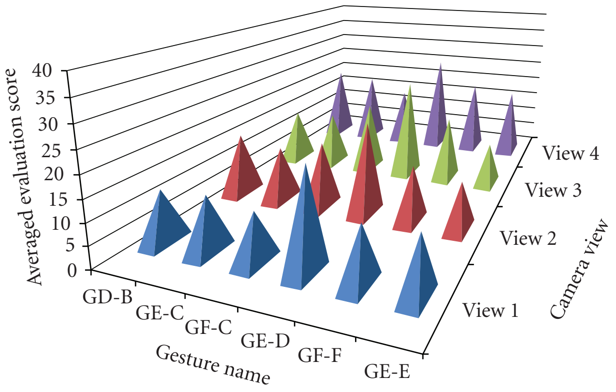

Figure 20: Averaged evaluation scores when the gesture GI-D(GE-D) is input to the system.

Table 5: Average recognition rates for ExperimentsII and III (%).

Exp.	Q_0	Q_1	Q_2	Q_3	Q_4	Ave.
II	98.0	81.8	80.1	88.2	91.8	88.0
III	99.7	98.3	89.4	83.9	98.2	93.9
Ave.	98.9	90.1	84.8	86.1	95.0	91.0

are shown in Figure 12, for the gestures in group H are shown in Figure 13, and for the gestures in group I are shown in Figure 14.

In the above experiments, each recognition rate is computed by dividing "the rate of correct answers" by "the rate of correct answers" plus "the rate of wrong answers." "The rate of correct answers" refers to the ratio of the number of correct recognition to the number of processed image frames, which is calculated only for the correct gesture class. On the other hand, "the rate of wrong answers" refers to the ratio of the number of wrong recognition to the number of processed image frames, which is calculated for all gesture classes except the correct gesture class. In this way, a recognition rate is calculated that reflects the occurrence of incorrect recognition during the evaluation. The recognition rates shown in the figures and tables are the averaged values given by the above calculation about 10 testing samples of each gesture in Experiment I and 20 testing samples in Experiments II and III.

Table 6: Classification by view dependency.

Experiment I	
Group A	
Independent	GA-A, GA-B, GA-C GA-D, GA-E, GA-F
Dependent	None
Group B	
Independent	GB-A, GB-B, GB-C GB-D, GB-E, GB-F
Dependent	None
Group C	
Independent	GC-A GC-B, GC-C GC-D GC-E, GC-F
Dependent	None
Experiment II	
Group D	
Independent	None
Dependent	GD-A, GD-B, GD-C GD-D, GD-E, GD-F
Group E	
Independent	GE-B, GE-E
Dependent	GE-A, GE-C, GE-D GE-F
Group F	
Independent	GF-C, GF-D
Dependent	GF-A, GF-B, GF-E GF-F
Experiment III	
Group G	
Independent	GD-A
Dependent	GD-E, GE-B, GF-E GF-D, GF-A
Group H	
Independent	GD-C, GE-F
Dependent	GE-A, GD-F, GD-D GF-B
Group I	
Independent	GE-D, GF-C
Dependent	GD-B, GE-C, GF-F GE-E

5. Discussion

5.1. Performance on ViHASi Database. As shown in Table 4, each view's average recognition rate for Groups (A, B, and C) exceeds 99.0 (%). And the average recognition rate's dependency on views is very small. This suggests that the selected 18 gestures in Groups (A, B, and C) are so distinctive that any one of the views is enough for correct recognition. It should be noted here that each view's contribution can never be evaluated without performing multiview recognition. On the other hand, the average recognition rate for the integration agent Q_0 constantly reaches 100.0 (%). Above results toward the public image database demonstrate the fundamental strength of our gesture recognition method.

5.2. Performance on Our JSL Database. As shown in Table 4, the overall average recognition rate reaches 88.0 (%) for Groups (D, E, and F) and 93.9 (%) for Groups (G, H, and I). Compared with 99.9 (%) for Groups (A, B, and C), the figure is relatively low. It should be noted that the results for Groups (A, B, and C) are obtained by using only standard samples, while the results for Groups (D, E, F, G, H, and I) are obtained by using similar samples. Similar samples are collected by letting one person repeat the same gesture for 20 times. Since no person can perfectly replicate the same gesture, similar samples are all different spatially and temporally. Notwithstanding, the average recognition rate

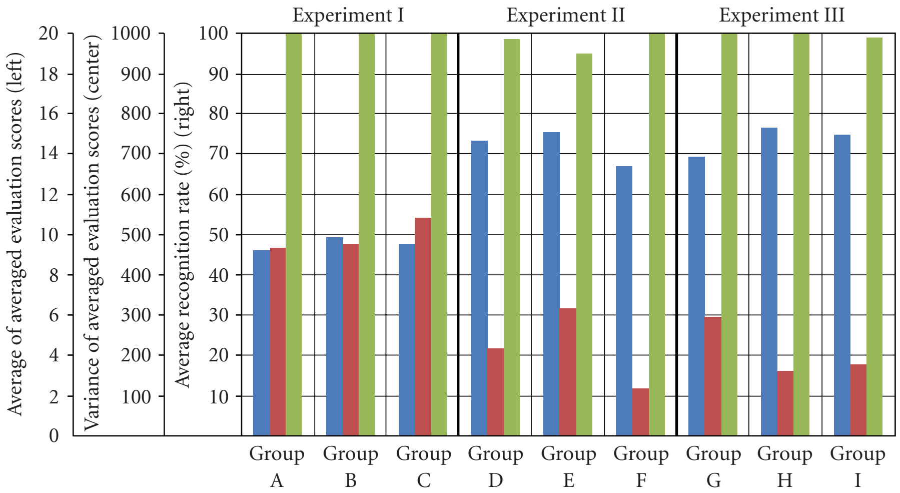

Figure 21: Average recognition rate and average/variance of averaged evaluation scores for each group.

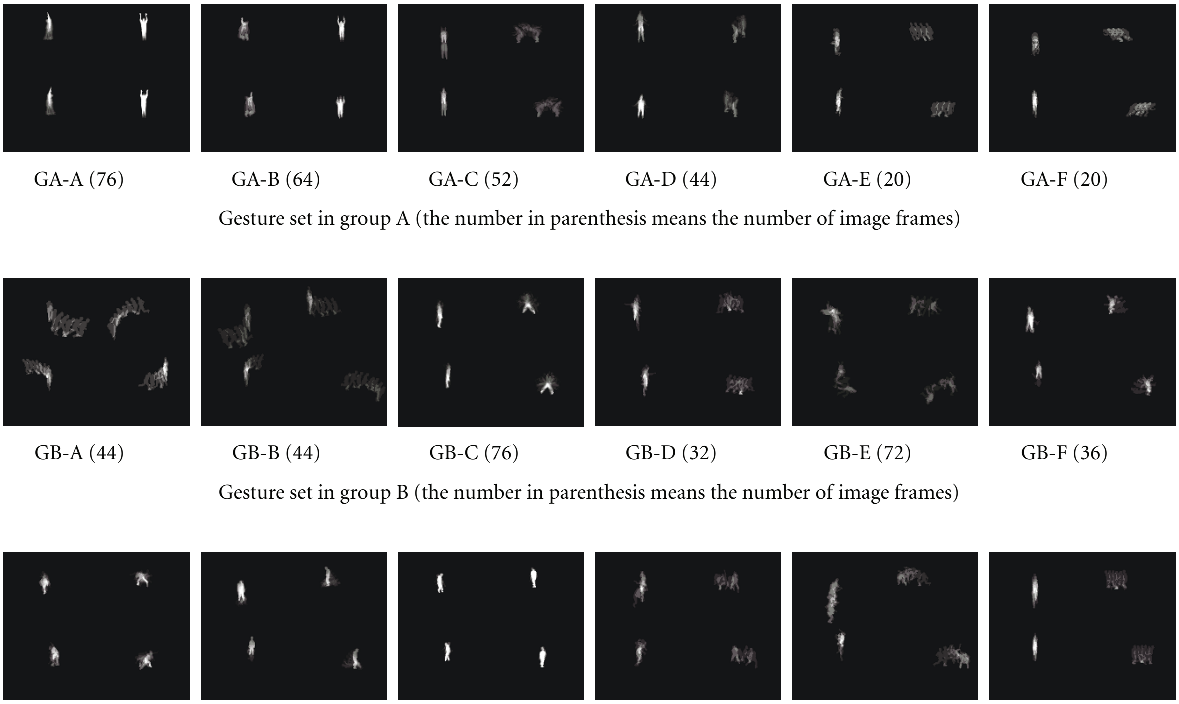

GA-A (76) GA-B (64) GA-C (52) GA-D (44) GA-E (20) GA-F (20)

Gesture set in group A (the number in parenthesis means the number of image frames)

GB-A (44) GB-B (44) GB-C (76) GB-D (32) GB-E (72) GB-F (36)

Gesture set in group B (the number in parenthesis means the number of image frames)

GC-A (76) GC-B (36) GC-C (80) GC-D (52) GC-E (40) GC-F (32)

Gesture set in group C (the number in parenthesis means the number of image frames)

Figure 22: Trace images of gestures adopted in Experiment I.

for the integration agent Q_0 reaches 98.0 (%) for Groups (D, E, and F) and 99.7 (%) for Groups (G, H, and I). These figures are comparable to the results for Groups (A, B, and C). Considering the greater variability in the testing samples, the integration agent Q_0 performs quite well for Groups (D, E, F, G, H, and I). Actually, the integration agent Q_0 performs best for our JSL image database as shown in Table 5. In our view, these are the indication of swarm intelligence [19–22] since the integration agent Q_0 outperforms individual recognition agent without any mechanisms for centralized control. Regarding the performance of individual recognition agent, the frontal view Q_1 performs best for Groups (F and H), while the side view Q_4 performs best for Groups (D, E, G, and I) as shown in Table 4. Interestingly, best recognition performance is not always achieved by frontal views, suggesting that the best view can depend on target gesture sets.

5.3. Classification by View Dependency. When the difference between the maximal and the minimal average recognition

GD-A (21) GD-B (26) GD-C (18) GD-D (37) GD-E (27) GD-F (23)

Gesture set in group D (the number in parenthesis means the number of image frames)

GE-A (23) GE-B (21) GE-C (19) GE-D (20) GE-E (36) GE-F (21)

Gesture set in group E (the number in parenthesis means the number of image frames)

GF-A (12) GF-B (28) GF-C (15) GF-D (22) GF-E (20) GF-F (25)

Gesture set in group F (the number in parenthesis means the number of image frames)

GG-A (GD-E) GG-B (GE-B) GG-C (GF-E) GG-D (GF-D) GG-E (GD-A) GG-F (GF-A)

Gesture set in group G (the name in parenthesis means the original gesture name)

GH-A (GD-C) GH-B (GE-A) GH-C (GD-F) GH-D (GD-D) GH-E (GF-B) GH-F (GE-F)

Gesture set in group H (the name in parenthesis means the original gesture name)

GI-A (GD-B) GI-B (GE-C) GI-C (GF-C) GI-D (GE-D) GI-E (GF-F) GI-F (GE-E)

Gesture set in group I (the name in parenthesis means the original gesture name)

Figure 23: Trace images of gestures adopted in Experiments II and III.

rate of each gesture in Figures 6, 7, 8, 9, 10, 11, 12, 13, and 14 does not fall within 10 (%), let us say "the gesture exhibits view dependency." The classification results based on this criterion for all gesture groups are summarized in Table 6. Regarding the Groups (A, B, and C), no gesture exhibits view dependency. On the other hand, 14 out of 18 gestures (→ 78 (%)) in Groups (D, E, and F) exhibit view dependency. And 13 out of 18 gestures (→ 72 (%)) exhibit view dependency regarding the Groups (G, H, and I). There is a striking difference between the Groups (A, B, and C) and the Groups (D, E, F, G, H, and I) with respect to view dependency. This suggests that the gestures in Groups (D, E, F, G, H, and I) are not so distinctive that all views are necessary for correct recognition. By utilizing the output of each recognition agent, the integration agent Q_0 exhibits better performance than individual recognition agent. Moreover, the classification results on 7 out of 18 gestures (→ 39 (%)) in the Groups (D, E, and F) have changed in the Groups (G, H, and I). This implies that view dependency can be affected by the combination of the target gestures.

5.4. Analysis on View Dependency. Figure 15 shows the typical response of the averaged evaluation scores when samples in Groups (A, B, and C) are tested. Figure 18 shows the typical response of the averaged evaluation scores when samples in Groups (D, E, F, G, H, and I) are tested. Averaged evaluation scores are computed by taking an average of evaluation scores when all testing samples are sequentially tested. For the samples in Groups (A, B, and C), the distinction between the correct gesture class and the wrong gesture classes is very clear. On the other hand, for the samples in Groups (D, E, F, G, H, and I), wrong responses are rampant and they vary depending on the views. This can also be confirmed in Figures 16, 17, 18, 19, and 20. Regarding the view dependency, Figures 16 and 19 show the case in which the view dependency increases. And Figures 17 and 20 show the case in which the view dependency decreases. Above results imply that the change in the combination of target gestures affects the distinctiveness from respective views, which can cause a change in view dependency.

5.5. Quantitative Difference between ViHASi and Our JSL Image Database. Figure 21 shows the average recognition rate and the average/variance of averaged evaluation scores for each group. Apparently, there is little correlation between the average recognition rate and the average/variance of averaged evaluation scores. But the variance of averaged evaluation scores for Experiment I is larger than that of Experiments II and III. And the average of averaged evaluation scores for Experiment I is smaller than that of Experiments II and III. Above results seem to have been brought about by the following reasons. In Experiment I, only standard samples in ViHASi image database are used for both the learning and the test. On the other hand, in Experiments II and III, only one standard sample and one similar sample in our JSL image database are used for the learning. And the similar samples that are evidently less distinct and more ambiguous than the samples in ViHASi image database are used during the test. Nevertheless, the results of the integration agent for our JSL image database are comparable to the results for ViHASi image database, suggesting that our approach requires only a small amount of samples for learning. The greatest merit of multiview approach lies in that it can capture multiple samples from different views at the same time. This reduces the user's burden before using the recognition system.

6. Summary

In this paper, a framework is proposed for multiview recognition of human gestures by real-time distributed image processing. In our framework, recognition agents run in parallel for different views, and the recognition results are integrated on-line and in real-time. In the experiments, the proposed approach is evaluated by using two kinds of image databases: (1) public ViHASi image database and (2) original JSL image database. By examining recognition rates of each gesture for each view, we found gestures that exhibit view dependency and the gestures that do not. And the most suitable view for recognition varied depending on the gestures in each of nine groups. More importantly, some gestures changed view dependency by changing the combination of target gestures. Therefore, the prediction of the most suitable view is difficult, especially when the target gesture sets are not determined beforehand as in the case of user-defined gestures. On the whole, the integration agent demonstrated better recognition performance than individual fixed-view recognition agent. The results presented in this paper clearly indicate the effectiveness of our swarm-based approach in multiview gesture recognition. Future work includes the application of our approach to many view gesture recognition in sensor network environment.

References

[1] M. Weiser, "Hot topics-ubiquitous computing," *Computer*, vol. 26, no. 10, pp. 71–72, 1993.

[2] T. Matsuyama and N. Ukita, "Real-time multitarget tracking by a cooperative distributed vision system," *Proceedings of the IEEE*, vol. 90, no. 7, pp. 1136–1149, 2002.

[3] R. Liu, Y. Wang, H. Yang, and W. Pan, "An evolutionary system development approach in a pervasive computing environment," in *Proceedings of International Conference on Cyberworlds (CW '04)*, pp. 194–199, November 2004.

[4] J. Yamato, J. Ohya, and K. Ishii, "Recognizing human action in time-sequential images using hidden Markov model," in *Proceedings of IEEE Computer Society Conference on Computer Vision and Pattern Recognition (CVPR '92)*, pp. 379–385, Champaign, Ill, USA, June 1992.

[5] C. R. Wren, A. Azarbayejani, T. Darrell, and A. P. Pentland, "Pfinder: real-time tracking of the human body," *IEEE Transactions on Pattern Analysis and Machine Intelligence*, vol. 19, no. 7, pp. 780–785, 1997.

[6] A. Corradini, "Dynamic time warping for off-line recognition of a small gesture vocabulary," in *Proceedings of IEEE ICCV Workshop on Recognition, Analysis, and Tracking of Faces and Gestures in Real-Time Systems*, pp. 82–89, July 2001.

[7] P. Dreuw, T. Deselaers, D. Rybach, D. Keysers, and H. Ney, "Tracking using dynamic programming for appearance-based sign language recognition," in *Proceedings of the 7th International Conference on Automatic Face and Gesture Recognition (FGR '06)*, pp. 293–298, April 2006.

[8] Z. Hang and R. Qiuqi, "Visual gesture recognition with color segmentation and support vector machines," in *Proceedings of the International Conference on Signal Processing (ICSP '04)*, vol. 2, pp. 1443–1446, Beijing, China, September 2004.

[9] S.-F. Wong and R. Cipolla, "Continuous gesture recognition using a sparse Bayesian classifier," in *Proceedings of International Conference on Pattern Recognition*, vol. 1, pp. 1084–1087, September 2006.

[10] U. C. Jung, H. J. Seung, D. P. Xuan, and W. J. Jae, "Multiple objects tracking circuit using particle filters with multiple features," in *Proceedings of International Conference on Robotics and Automation*, pp. 4639–4644, April 2007.

[11] C. Wan, B. Yuan, and Z. Miao, "Model-based markerless human body motion capture using multiple cameras," in *Proceedings of IEEE International Conference on Multimedia and Expo*, pp. 1099–1102, July 2007.

[12] M. Ahmad and S.-W. Lee, "HMM-based human action recognition using multiview image sequences," in *Proceedings of International Conference on Pattern Recognition (ICPR '06)*, vol. 1, pp. 263–266, September 2006.

[13] A. Utsumi, H. Mori, J. Ohya, and M. Yachida, "Multiple-human tracking using multiple cameras," in *Proceedings of the 3rd IEEE International Conference on Automatic Face and Gesture Recognition (FGR '98)*, pp. 498–503, April 1998.

[14] T. Kirishima, Y. Manabe, K. Sato, and K. Chihara, "Multi-rate recognition of human gestures by concurrent frame rate control," in *Proceedings of the 23rd International Conference Image and Vision Computing New Zealand (IVCNZ '08)*, pp. 1–6, November 2008.

[15] S. Abbasi and F. Mokhtarian, "Automatic view selection in multi-view object recognition," in *Proceedings of the 15th International Conference on Pattern Recognition (ICPR '00)*, pp. 13–16, September 2000.

[16] L. E. Navarro-Serment, J. M. Dolan, and P. K. Khosla, "Optimal sensor placement for cooperative distributed vision," in *Proceedings of IEEE International Conference on Robotics and Automation (ICRA '04)*, pp. 939–944, July 2004.

[17] T. Kirishima, K. Sato, and K. Chihara, "Real-time gesture recognition by learning and selective control of visual interest points," *IEEE Transactions on Pattern Analysis and Machine Intelligence*, vol. 27, no. 3, pp. 351–364, 2005.

[18] H. Ragheb, S. Velastin, P. Remagnino, and T. Ellis, "ViHASi: virtual human action silhouette data for the performance evaluation of silhouette-based action recognition methods," in *Proceedings of the 2nd ACM/IEEE International Conference on Distributed Smart Cameras (ICDSC '08)*, pp. 1–10, Palo Alto, Calif, USA, September 2008.

[19] M. G. Hinchey, R. Sterritt, and C. Rouff, "Swarms and swarm intelligence," *Computer*, vol. 40, no. 4, pp. 111–113, 2007.

[20] L. M. Fernández-Carrasco, H. Terashima-Marín, and M. Valenzuela-Rendón, "On the path towards autonomic computing: combining swarm intelligence and excitable media models," in *Proceedings of the 7th Mexican International Conference on Artificial Intelligence (MICAI '08)*, pp. 192–198, October 2008.

[21] P. Saisan, S. Medasani, and Y. Owechko, "Multi-view classifier swarms for pedestrian detection and tracking," in *Proceedings of the IEEE Computer Society Conference on Computer Vision and Pattern Recognition (CVPR '05)*, p. 18, San Diego, Calif, USA, June 2005.

[22] M. Scheutz, "Real-time hierarchical swarms for rapid adaptive multi-level pattern detection and tracking," in *Proceedings of the IEEE Swarm Intelligence Symposium (SIS '07)*, pp. 234–241, April 2007.